Available online at www.sciencedirect.com
SCIENCE DIRECT
Cement and Concrete Research 36 (2006) 791 – 800
Cement and Concrete Research

In-situ monitoring the realkalisation process by neutron diffraction: Electroosmotic flux and portlandite formation

Marta Castellote [a,*], Irene Llorente [a], Carmen Andrade [a], Xavier Turrillas [a], Cruz Alonso [a], Javier Campo [b]

[a] Institute of Construction Sciences "Eduardo Torroja" (IETcc), CSIC, 28033, Madrid, Spain
[b] Institute of Science of Materials of Aragón (ICMA), CSIC, 50005, Zaragoza, Spain

Received 10 February 2005; accepted 7 November 2005

Abstract

Even though the electroosmotic flux through hardened cementitious materials during laboratory realkalisation trials had been previously noticed, it has never been in-situ monitored, analysing at the same time the establishment of the electroosmotic flux and the microstructure changes in the surroundings of the rebar. In this paper, two series of cement pastes, cast with CEM I and CEM I substituted in a 35% by fly ash, previously carbonated at 100% CO_2, were submitted to realkalisation treatments followed on line by simultaneous acquisition of neutron diffraction data. As a result, it has been possible to confirm the electroosmosis as the driving force of carbonates towards the rebar and to determine the range of pH in the anolyte in which most of the relevant electroosmotic phenomena takes place. On the other hand, the behaviour of the main crystalline phases involved in the process has been monitored during the treatment, with the precipitation of portlandite as main result.

Keywords: Realkalisation; Neutron diffraction; Portlandite formation; Electroosmotic flux

1. Introduction

Realkalisation is a relatively new electrochemical technique for repairing structures damaged by rebar corrosion due to carbonation. The treatment consists in applying continuous current between the rebar (acting as negative electrode or cathode) and an auxiliary external electrode, (in a carbonate solution and connected to the positive pole of the power supply) with the aim of restoring the alkalinity of the concrete loss by the carbonation process. This restoration seems to be primarily provided by the generation of OH^- at the rebar level, through the reaction of water electrolysis at the steel acting as the cathode. However, it has been claimed [1–5] that carbonate ions also penetrate towards the rebar. Being the charge of carbonates negative, this penetration towards the cathode does not seem feasible unless other mechanisms, different than migration forces, operate.

At the surface of a solid in contact with an electrolyte, in general, a difference of potential is developed. When one of these phases (solid or liquid) is caused to move tangentially past the second phase, a number of phenomena, which are grouped under the generic name of "electrokinetic effects" can develop. The zeta-potential is the average potential in an imaginary surface which is considered to lie close to the solid surface and where the fluid is stationary (surface of shear), and is the key parameter in the establishment of the electrokinetic effects. When the solid remains stationary and the liquid moves in response to an applied electrical field this is called electroosmosis [6], which is the case of concrete submitted to the electrochemical treatment of realkalisation.

In [5], the application of the theoretical equations of electroosmosis to concrete was undertaken, and quite recently, the authors were able to observe and quantify the electroosmotic flux through hardened carbonated CEM I concrete [7] and reported laboratory trials on carbonated CEM I mortars [8]. In addition, the influence of the external solution (concentration of Na_2CO_3 in the anodic compartment) was analysed resulting that the pH in the anolyte seemed to be one determining parameter on the zeta potential and consequently on the establishment of the electroosmotic flux [8]. However, a realkalisation treatment has never been in-situ monitored,

* Corresponding author. Tel.: +34913020440; fax: +34913020700.
E-mail address: martaca@ietcc.csic.es (M. Castellote).

0008-8846/$ - see front matter © 2005 Elsevier Ltd. All rights reserved.
doi:10.1016/j.cemconres.2005.11.014

analysing at the same time the development of the electroosmotic flux and the microstructural variations in the surroundings of the rebar. This has been undertaken in the present paper, where realkalisation treatments on cement pastes cast with two different binders were followed on line by simultaneous acquisition of diffraction data at the D20 instrument of the Institute Max von Laue-Paul Langevin (ILL), in Grenoble, France.

2. Experimental

2.1. Materials and preparation of specimens

Two series of cement pastes were prepared by hand mixing cement with deuterated water from 99.95% purity to a w/c ratio of 0.5. The first series, mix A, used Ordinary Portland Cement of type I/45A/SR-MR, composed of a 95% of clinker type I and a 5% of lime, whose chemical analysis is shown in Table 1. The second series, mix B, was prepared using the same cement but substituted in a 35% by fly ash, whose composition is also given in Table 1.

The specimens were cast in cylindrical moulds of 2.2 cm of internal diameter and 6 cm length, with a high strength cold drawn steel for pre-stressed structures perpendicularly to the axis of the cylinder of the specimen (see Fig. 1).

Prior to the realkalisation tests, after 7 days of curing in a high humidity chamber (>95% RH) and subsequent drying, the specimens were carbonated at 65% RH, 20±2 °C, and 100% CO_2 concentration. The specimens were held in the chamber for one month until negligible increase in weight was recorded. The fully carbonated state was confirmed by breaking duplicate specimens and spraying phenolpthalein indicator on the fresh fractures.

2.2. Techniques and procedures

The experimental set up of the test is shown in Fig. 2. A ponding was glued on the top of the cylinder of cement paste and was filled with a solution of Na_2CO_3 1 M prepared with ordinary, non-deuterated, distilled water. The experiment was designed in this way with the hypothesis that if electroosmotic flux took place, as it will came from the anodic compartment, an abrupt increase in the background of the diffraction patterns should occur due to incoherent scattering of the hydrogen of the water.

An activated titanium mesh was introduced in the carbonate solution compartment and was electrically connected to the positive side of the power supply. The rebar embedded in the sample was used as negative electrode. A voltage drop of 72 V DC was applied and the current passing through the specimen was monitored. In the case of mix A, after 9 h running the test, the current was switched off without dismantling the device, and after a delay of about 7 h, the voltage drop was connected again for 4 h more. After that time, the voltage was again switched off and the specimen was taken out of the neutron beam. The specimen was stored in laboratory environment for 72 h, then, the anolyte chamber was filled in again with fresh solution of Na_2CO_3 1 M and the test was allowed to run for 12 h more. In mix B (CEM I+FA), the carbonate solution was completely depleted in the anolyte chamber after approximately 6 h and the test was left running for 3 other hours. After this period, the anolyte chamber was filled in with fresh solution of Na_2CO_3 1 M and the test was allowed to run for 5 h more. A summary of the experimental details is given in Table 2.

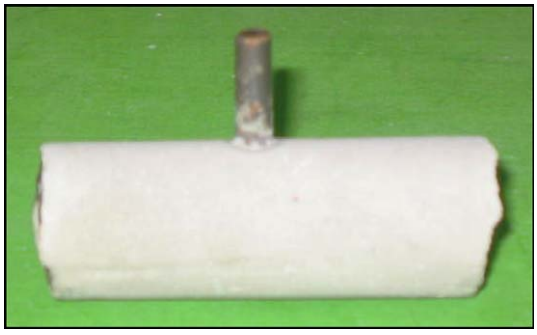

Fig. 1. Specimens used for the realkalisation experiments.

The electrical treatment was followed on line by simultaneous acquisition of diffraction data at the D20 instrument of the Institute Max von Laue-Paul Langevin (ILL), in Grenoble, France. The neutron diffraction data were collected continuously storing the detector counts every 120 s, exploring an angular domain in 2θ from 10° to 150°. The neutron beam had a rectangular section of 8×12 mm^2 and was centred in the middle of the sample, as shown in Fig. 2, monitoring 4 mm of the rebar and the 4 mm of the area of the sample closer to the negative electrode.

To exactly calibrate the wavelength, a powder of Si furnished by the NBS (National Bureau Standard) was used. The diffraction pattern of this standard was refined by Rietveld analysis and a wavelength of 1.28 was found. This wavelength was used in the subsequent measurements.

Additionally, in the case of mix B, after the voltage drop was switched off at the end of the experiment, the portion of the sample between the electrodes was scanned by dividing it into five different zones, about 5 mm long each. The adjacent region to the negative electrode was named Z1, and the opposite one, in contact with the positive one, Z5.

Table 1
Chemical analysis of the cement and fly ash used

	L.I.	I.R.	SiO_2	Al_2O_3	Fe_2O_3	CaO	MgO	SO_3	Cl^-	Na_2O	K_2O	Free CaO
Cement	1.7	0.7	20.2	2.37	4.1	65.84	1.85	3.8	0.02	0.11	0.65	1.5
Fly ash	2.58	–	48.71	25.18	5.18	12.09	1.61	0.43	–	0.61	3.28	0.15

L.I.: Loss on ignition; I.R.: Insoluble residue.

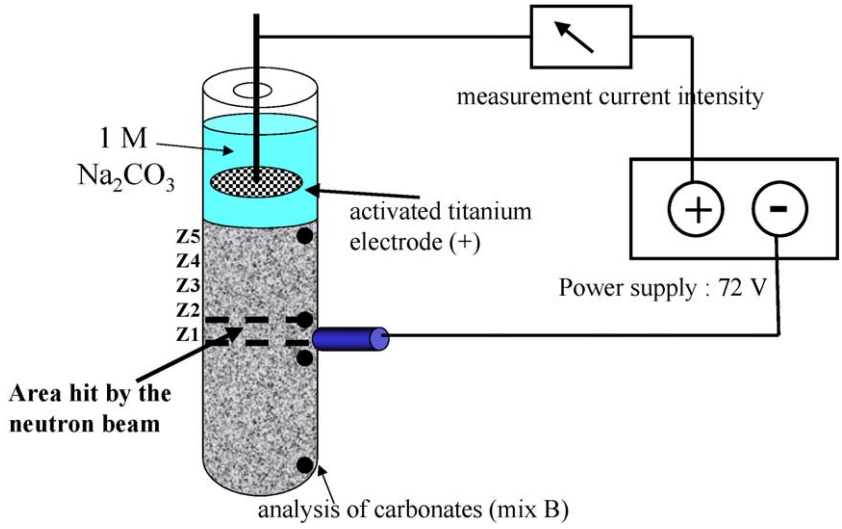

Fig. 2. Scheme of the set up of the experiment.

After the realkalisation experiments, out of the neutron beam, the samples were cut according to a plane perpendicular to the rebar and were treated in the following way:

- Phenolftaleine was sprayed on the fresh fracture in order to study the realcalised zones of the specimen.
- In the case of mix B, four parts of the specimen, of about 2 mm length, were also taken off and the carbonates analysed following the leaching procedure recommended for chlorides in [9] by water extraction. The location of these samples are given in Fig. 2, as black spots, where it is shown that they were taken close to the negative electrode towards both ends of the cylinders and close to the ends of the cylinder (one of them corresponding to the positive side).
- A part of the specimen between the electrodes was cut along planes parallel to the position of the electrodes, obtaining five different portions (of approximately 5 mm each), corresponding to different areas in the specimen (Z1 to Z5 in Fig. 2). These portions, as well as the reference sample, without treatment, were analysed by Mercury Intrusion Porosimetry (MIP) in order to study the residual state of the specimens.

The powder diffraction patterns have been analysed by a standard procedure. Crystalline phases were identified by a search-match manual procedure and selected peaks for calcite, vaterite and portlandite were fitted to Gaussian curves for the whole series. The variation of intensity of a chosen reflection for a particular phase along the experiment (related with the concentration) has been used to monitor concentration changes.

Table 2
Summary of the steps in the realkalisation process for each mix

	Step	Duration (h)	Solution in the anolyte	Voltage (V)
Mix A (CEM I)	a)	9	Yes (fresh solution)	72
	b)	7	Yes	0
	c)	4	Yes	72
	d)	72	No (specimen out of the neutron beam)	0
	e)	12	Yes (fresh solution)	72
Mix B (CEM I+FA)	a)	6	Yes (fresh solution)	72
	b)	3	No	72
	c)	5	Yes (fresh solution)	72

3. Results

3.1. Analysis of the diffraction patterns during the treatment

Provided that the specimens were cast with deuterated water, and the Na_2CO_3 solution was prepared with ordinary distilled water, if electroosmotic flux took place there would be an abrupt increase in the background of the diffraction patterns due to incoherent scattering of the H of the water.

The evolution of the integration of the backgrounds of the diffraction patterns (normalised intensity to unity at the low 2θ region, where no peaks appear), is presented in Fig. 3(a–b) for the two mixes tested. In Fig. 3, the points where the jumps in the background imply the establishment of electroosmotic flux have been marked with arrows. In these figures, the evolution of the electric current during the experiments have also been depicted, in order to confirm the parallelism previously detected [7] between the sudden increase in the current and the electroosmotic flux.

Concerning the experiment for mix A, at the beginning of the experiment (step a), the current is very small. At this point there is a small decrease of the background, due to the consumption of water due to electrolysis at the rebar level. After that, the background and the current seem to start to increase when step b) is reached and the power supply is switched off. When the voltage drop is connected again (step c), the tendency in the current curve goes on from the same point, that was reached when the power supply was disconnected, to an abrupt increase in the current is registered. This increase is due to the drag of water from the anodic compartment when the electroosmotic flux is established, as can be derived from the corresponding increase in the background counts. Afterwards, the specimen is taken out of

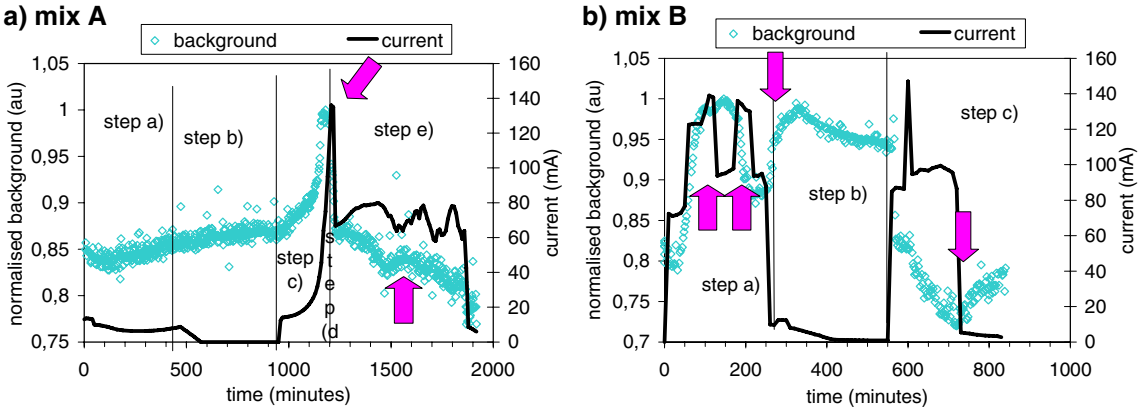

Fig. 3. (a–b): Evolution of the normalised background (in arbitrary units) and the electrical current (mA) passing through the specimens during the realkalisation treatments.

the beam (step d) and after 72 h, the experiment was allowed to proceed (step e). During this last step, the background decreases quickly due to the high electrical current passing that consumes water at the rebar level. According to the current passing in the last stages of the experiment, there could have been three other small electroosmotic processes; however, only one has been clearly detected at the rebar level by an increase in the background (as marked by the arrow).

Concerning the experiment for mix B, after the small decrease of the background due to the initial consumption of water at the rebar level, the current starts to increase quite quickly and so does the background, which implies the establishment of the electroosmotic flux very early in this experiment. According to the current curve, there is a kind of double electroosmotic processes; however, the second one cannot be detected in the background level provided that it has already reached its maximum value, that is to say, the specimen is completely full of solution in the surroundings of the steel. Then, the high current passing goes on consuming the excess of water around the rebar and the background starts to decrease when there is another electroosmotic process which consumes all the solution in the anodic compartment. The water reaches the rebar but there is a loss of the electrical contact with the positive electrode (due to the lack of anolyte) and, therefore, the current goes to zero (step b). When filling again the anodic compartment with fresh solution (step c), the current increases and the background decreases due to the electrolysis of water. When water at the rebar level has almost been depleted, a new episode of electroosmotic flux starts to take place. Therefore, in this experiment, four electroosmotic peaks have been detected.

Concerning the crystalline phases, the analysis of the neutron diffraction patterns has allowed to identify, as expected, calcite as the main crystalline phase in the samples. In addition, vaterite has also been identified, in lesser extent, as previously reported by other authors [10] irrespective of the percentage of CO_2 used to in the treatment of carbonation. For both mixes, at the latest stages of the treatment, the presence of portlandite has also been noticed. Selected peaks of these phases (reflexion 104 for calcite, 111/021 for vaterite and 101/011 for portlandite) were chosen because their isolation and intensity and were fitted to Gaussian curves for the whole series. The variation of the heights of these reflections along the experiment was used to monitor concentration changes and it is given in Fig. 4(a–b), where the evolution of the normalised height as a function of the time is depicted.

It has to be pointed out that the absolute amount of each of these phases cannot be deduced from Fig. 4, as the scale of the *Y* axis has been normalized, for each phase to the maximum

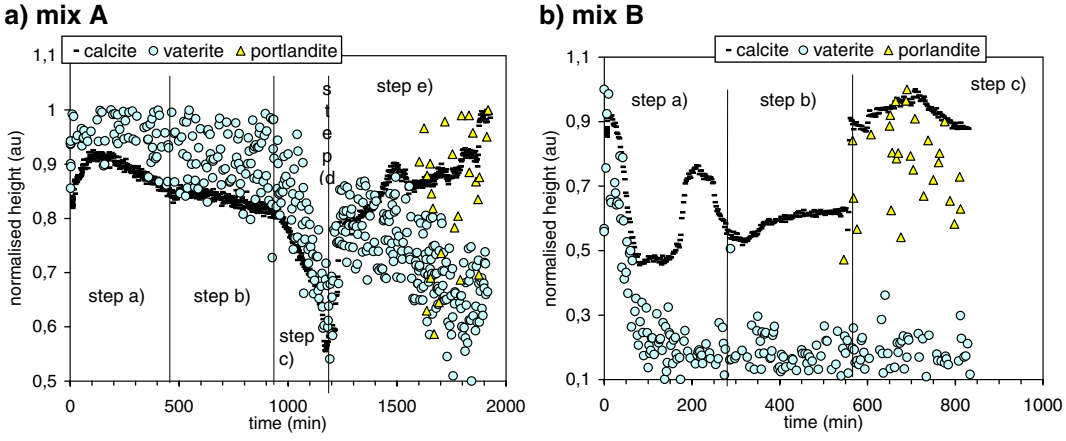

Fig. 4. (a–b): Evolution of the normalised height as a function of the time for a) mix A and b) mix B.

value, taken as 1. In fact, the amount of portlandite formed is very small, not comparable with the amount of remaining calcite, as can be derived from Fig. 5, where a detail of the initial diffraction pattern (prior the treatment) and the final one (after the treatment) for mix B is given.

3.2. Analysis of the specimen after the realkalisation treatment on the neutron beam

After the experiment, for mix B, diffraction patterns were taken in 6 zones covering the rebar and the whole specimen between anolite and catholite. The normalized counts for the background and heights, for the three monitored phases (calcite, vaterite and portlandite), along the different zones of the specimen are given in Fig. 6(a–b), respectively.

From Fig. 6-a it can be deduced that the background is higher in the zone closer to the rebar and it diminishes smoothly along the specimen reaching its minimum abruptly near the positive electrode. From Fig. 6-b, and taking into account that at the end of the test at the rebar level (negative side) the amount of calcite is about the same that before the experiment, (see Fig. 4-b), it can be deduced that precipitated calcite has been removed in the rest of the sample. The vaterite has dissolved mainly in the zones located close to the electrodes, having disappeared completely in the positive side. Portlandite has precipitated until about 12 mm from the centre of the steel.

3.3. Analysis of the specimen after the treatment out of the neutron beam

Once the samples were taken out of the neutron beam, after the realkalisation experiments, they were split in two halves in order to determine if they had been realkalised by spraying phenolptaleine indicator on the fresh fractures. The results are shown in Fig. 7, where it can be deduced that, for both mixes, the whole specimen between both electrodes has turned pink the indicator, which means realkalisation. Concerning the other part of the specimen, between the rebar and the end without

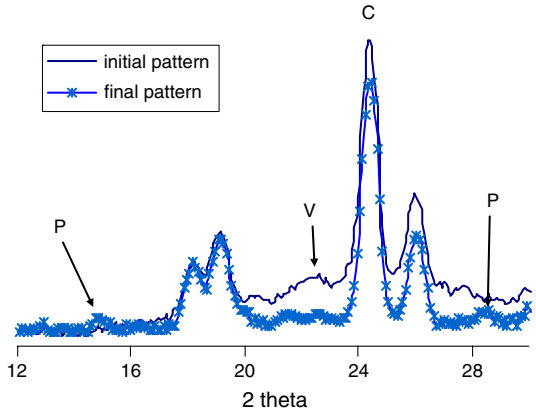

Fig. 5. Detail of the initial diffraction pattern (prior the treatment) and the final one (after the treatment) for mix B, where the peaks corresponding to P: Portlandite, C: Calcite and V: Vaterite have been marked.

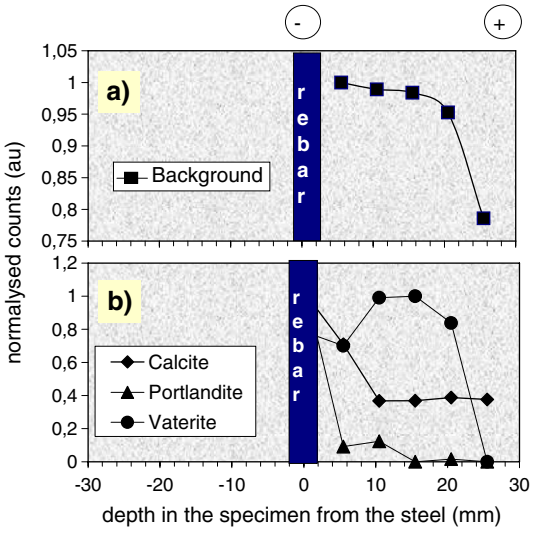

Fig. 6. (a–b): Normalised counts for a) the background and b) heights of the peaks for calcite, vaterite and portlandite, along the different zones of the specimen, mix B, between anolyte and catholite, after the realkalisation experiment.

electrode, as expected, only the zone closest to the rebar has been realkalised.

For mix B, the carbonates were analysed in four parts of the specimen of about 2 mm length, by water extraction [9]. The samples were taken close to the negative electrode towards both ends of the cylinders and close to the ends of the cylinder (one of them corresponding to the positive side) (see Fig. 2). It has to be pointed out that provided that the specimens were previously carbonated, the absolute amounts are not relevant, and therefore, the values obtained have been normalised to the maximum amount obtained.

The results are given in Fig. 8, from which it can be observed that the maximum amount of soluble carbonates in the sample can be found in the vicinity of the rebar, even more than close to the positive compartment. In addition, it can be deduced that no significant carbonates have passed behind the rebar.

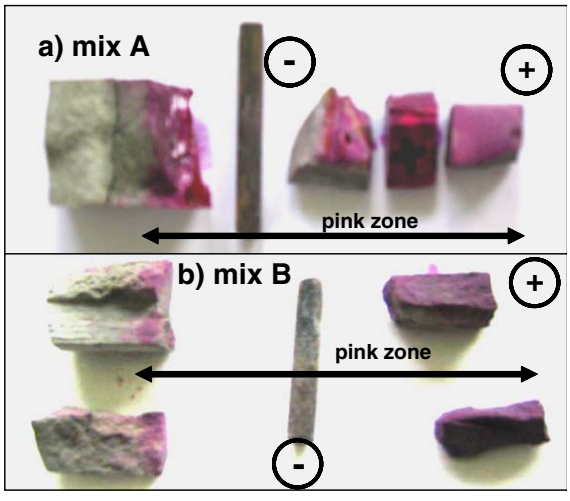

Fig. 7. (a–b): Results of the phenoftaleine sprayed on the fresh fracture of the samples after the realkalisation tests.

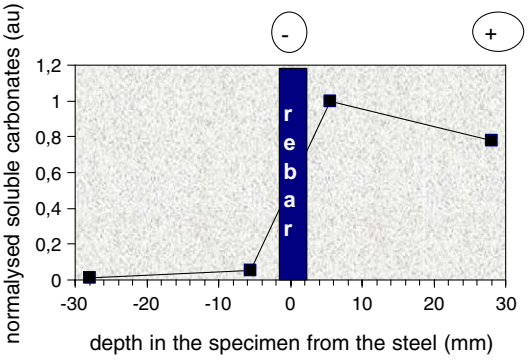

Fig. 8. Normalised water soluble carbonates, at different positions in the specimen of mix B, after the realkalisation experiment.

The results obtained from Mercury Intrusion Porosimetry are given in Table 3 where the total porosity (percent in volume) and the mean pore diameter are given.

In Table 3, it can be noticed that the electrical treatment induces important changes in porosity, differently distributed depending on the zone of the sample, but always showing larger mean pore diameter after the treatment. The most significant change for mix A is a high increase of the porosity in the positive side, zones 4 and 5. In the other part of the sample there are slight differences with respect to the untreated one, being these, the decrease and increase in the zones closest to the rebar and in the middle part of the sample, respectively. In mix B, there is about 20% of decrease in the porosity of the negative side of the sample and a slight increase of porosity in the rest of it. The differential pore size distributions presented in Fig. 9 allow performing a more detailed analysis.

Fig. 9(a–b) shows that in the case of mix A, there is an increase of porosity in all the zones of the specimen in the pore range higher than about 0.1 μm with a shift of the maximum exhibited by every sample towards higher pores. From 0.1 μm, the half part of the sample closer to the negative electrode starts to have smaller porosity than the untreated sample. In the zone between 0.2 and 0.03, the positive zones of the sample exhibit a maximum, much higher than the carbonated sample before the test and shifted towards higher pores. In the range of pores smaller than 0.03 μm, there is a decrease of porosity in every zone of the treated sample.

Table 3
MIP results of the samples

		Total porosity (% vol)	Mean pore diameter (μm)
Mix A	Carbonated before test	17.90	0.027
	Z1-negative	19.05	0.048
	Z2	16.67	0.048
	Z3	16.15	0.042
	Z4	25.73	0.057
	Z5-positive	25.19	0.052
Mix B	Carbonated before test	28.26	0.059
	Z1-negative	22.70	0.074
	Z2	30.67	0.083
	Z3	32.41	0.112
	Z4	30.51	0.077
	Z5-positive	30.91	0.070

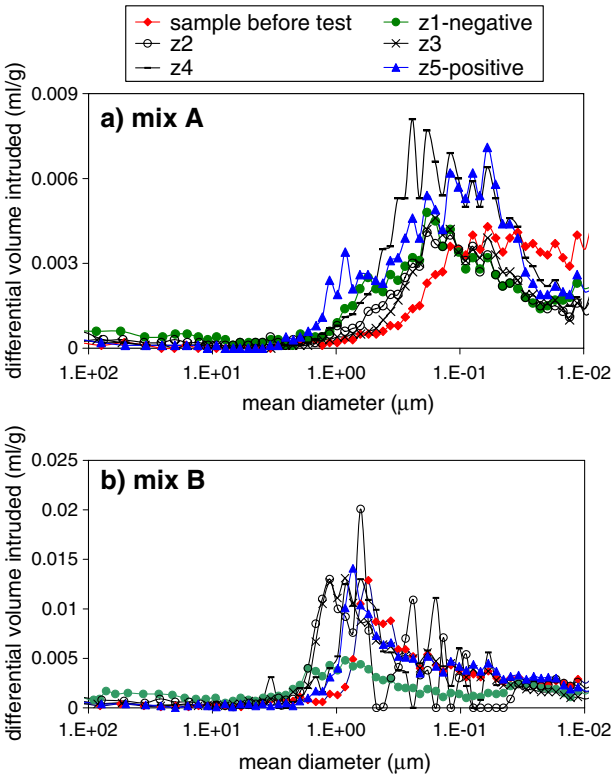

Fig. 9. (a–b). Differential pore size distribution of the samples. a) mix A (CEM I). b) mix B(CEM I+FA).

In the case of mix B, the trend is similar but with some differences. There is also a range of pores in which there is an increase of porosity for all zones of the specimen, but in this case, it is smaller than for mix A, extending to pores higher than 0.7 μm. The shift of the maximum towards higher pores (from 0.5 in the untreated sample to 1 in the case of the zones closer to the rebar) can be also detected. It can be pointed out the zone Z1, closer to the rebar, in the range between 0.7 and 0.05 μm, where the porosity is considerably smaller than for the rest of the zones, which exhibit a behaviour very similar to that of the reference untreated sample. For this mix, the range of pores smaller than 0.03 is not very significant even though there is also an small decrease of porosity in the treated sample.

Finally, it has to be remarked than for both mixes, the samples closer to the negative electrode have significantly higher values for the bigger pores (100–10 μm).

4. Discussion

4.1. Establishment of the electroosmotic flux

Recently, the authors quantified the electroosmotic flux through hardened carbonated concrete and mortar [7,8]. In agreement with these findings, even though the instantaneous flux of liquid could not be directly measured, the present results show the establishment of the electroosmotic flux through the specimens based on several facts:

The abrupt increase in the background of the diffraction patterns due to incoherent scattering of the H of the water must be due to the electroosmotic flux. The other possibility

(the water associated to the solvating sphere of Na^+ ions penetrating due to migration forces) would have implied an increase following a smooth process with a linear dependency with the charge density, as reported in previous realkalisation tests [7].

On the other hand, it is impossible for the carbonate or bicarbonate species, due to their negative charge, to move into the specimen by migration forces. In addition, from the results obtained in the analysis of soluble carbonates, there is no doubt that the carbonates enter the specimen through a mechanism different from that of diffusion. Provided that at the end of the test, the maximum concentration is reached at the level of the rebar, they must have entered by electroosmosis.

In order to determine the exact moment, and therefore the conditions, in the experiment in which the electroosmotic flux starts to develop, the derivative of the curve of the background in function of time has been calculated for both experiments. Therefore, in the inflexion points of the original curve towards higher slopes, a maximum appears in the derivative curve. The positions of these maximums give the points of establishment of the electroosmotic flux. The positive part of the derivative curves in function of the electrical charge density passed are depicted in Fig. 10, in which it can be observed that the scatter for mix A is higher than for mix B. Provided that the large scale in the graph may difficult the appearance of the peaks as simple lines, inside the graph a detail of the figure at low charge densities has also been depicted.

From this figure, it can be appreciated the large electroosmotic pulse that takes place for mix A at 1.3×10^6 C/m^2. Concerning the rest of the experiment, and looking at the shape of the peaks, two more peaks seem to be detected, at about 6×10^6 and 9.5×10^6 C/m^2, being the rest of the points attributed to the high scatter due to the small amount of flux established.

Concerning mix B, the three pulses previously identified can be clearly attributed to their corresponding charge densities, 8×10^5, $4{,}1\times10^6$ and 7×10^6 C/m^2. The first peak is considerably broader than the rest, which confirms the incorporation of two episodes of electroosmosis.

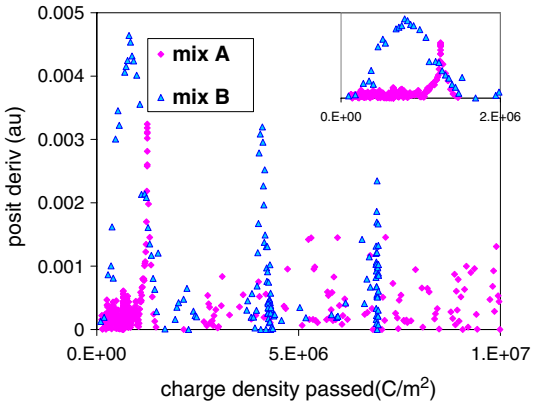

Fig. 10. Positive part of the derivative curves of the normalised background, in function of the electrical charge density. Detail for low charge densities passed.

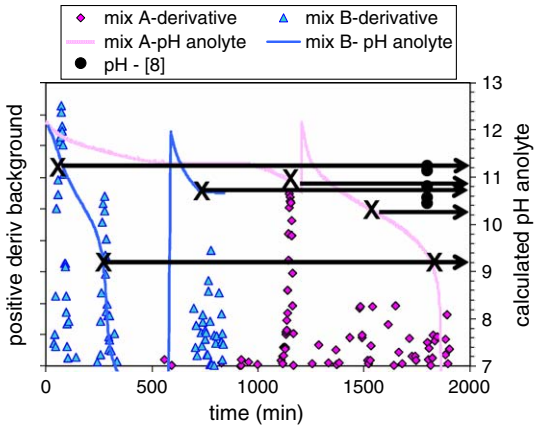

Fig. 11. Positive fraction of the derivative of the background (points) and pH calculated in the anolyte (lines) in function of the duration of the experiment. Data from reference [8] are also depicted.

In addition, these results confirm the fact, already pointed out in [8] that the establishment of the electroosmosis is not dependent exclusively on the charge density passed.

In [8], the values of zeta-potential for different experiments with different initial concentrations of Na_2CO_3 in the anolyte, for CEM I mortars, were correlated in function of the pH of the anolyte, calculating it by resolving the corresponding current-dependence-acid-basic system of chemical equations including dissociation and hydrolysis of Na_2CO_3 in the anolyte, reactions at the electrodes and migration of the different ions.

The pH in the anolyte has been calculated in the same way than in [8] for both tests, and their evolution has been depicted in Fig. 11 (as continuous lines with the scale in the right part of the figure). The increase in the pH up to the initial value of 12.2, means a replacement and/or filling of the anolyte with fresh solution. In this picture, the evolution of the positive fraction of the derivative of the background has also been represented (*Y* scale at the left part of the figure). In order to increase the clarity of the picture, taking out most of the scattered points, the bottom part of this *Y* scale has been removed.

From Fig. 11, the point of pH corresponding to the position of a maximum gives the calculated pH of the anolyte at which the pulse for dragging the solution takes place. The corresponding points for both mixes have been marked with arrows on the *Y* axis corresponding to pH. The values of pH at which the electroosmotic flux was clearly established in [8], have also been drawn in Fig. 11 (as a black points) for a better comparison. (For these points from [8], the values of time and of positive background do not apply; it refers only to pH).

From Fig. 11 it can be deduced that for carbonated cementitious matrixes CEM I+FA (mix B) the establishment of the electroosmotic flux starts very early in the experiment, may be due to the high initial current attributed to the high porosity of this mix. The point of the experiment related to the pulse of electroosmosis takes place when the pH of the anolyte has decreased until an approximate value of 11.3. In the case of

mix A, made from plain CEM I, the maximum value takes place at a pH of 10.9, very close to that of mix B and within the range found in [8], also for CEM I.

During the experiment, the concentration of the different species in the aqueous phase of the pores of the specimen is continuously changing, not only because of their own movement because of the action of the electrical field, but also due to the ions generated by the electrodic reactions. Therefore, when changing the solutions (steps e) and c) for mix A and B, respectively), the conditions of the electrical double layer in the walls of the pores is not the same than at the beginning, and the optimal point of pH in the anolyte compartment is not the same. From Fig. 11 it can be deduced that in both cases, these points are reached at lower values of pH. In the case of mix A, it takes place at about 10.5 of pH in the anolyte, and in the case of mix B, in this step, the maximum of the electroosmotic flux takes place at about 10.7. For both mixes, a new establishment of flux at about 9.5 of pH in the anolyte seems to take place.

Thus, it can be said that, for both mixes, and in agreement with reference [8], where different concentrations of Na_2CO_3 were tested, most of the relevant electroosmotic phenomena take place in the range of pH of the anolyte between 10.5 and 11.5. The point around 9.5 also has to be taken into account.

4.2. Calculation of the zeta-potential

In [8], the zeta-potentials were calculated in a differential way by monitoring continuously the electroosmotic flux. However, the data of this research do not allow performing these calculations. Nevertheless, the zeta-potentials have been calculated using the values of accumulated flux during the whole step of the experiment in which the passage of water takes place.

Calculation of the zeta-potentials has been made according to [6] with no assumptions on the potential distribution in the electrical double layer, providing it obeys Poisson's equation. Also, it has been assumed that the layer between the shear plane and the wall of the pore is unaffected by the applied electrical field and that the dielectric constant and the liquid viscosity coefficient retain their normal bulk values [6], as used in [5,7,8]. Thus, the values, calculated for steps c) and a) for the mixes A and B have been of −1.2 and −4 mV, respectively.

Therefore, it can be concluded that the zeta-potential of the electrical double layer in the pore walls of cement paste is more negative in case of adding fly ashes to the clinker than when using CEM I. The value found for CEM I is about ten times higher than the previously reported in [8], which as an hypothetical explanation is attributed to the different composition of the binders used. Some research is been carried out in order to explain this behaviour.

4.3. Microstructure changes in the paste

The duration of the realkalisation treatment does not seem to be the parameter of significance because the current is different for the different samples, at specific moments of the tests for the same sample, and even, during these experiments at some of the steps, the power supply has been switched off. Therefore, it seems that it is the electrical charge, as was stated previously [11–13], that has to be used to understand, define and control the treatment. Therefore, in order to make the picture of both mixes comparable, the evolution of both the normalised background and heights of the peaks of the crystalline species involved, is given in Fig. 12 for both mixes in function of the charge density passed (C/m^2).

During the realkalisation experiment, the concentration of every species in the aqueous phase of pores of the cement paste is continuously changing. This is due to its own movement under the action of the electrical field, to the dissolution or precipitation of solid phases, to the electroosmotic flux and also to the electrodic reactions. All these phenomena imply a change in the microstructure and phases of the paste.

Before the realkalisation treatment the specimens are carbonated, which means that the pH of the aqueous solution is below 9 with a considerable amount of precipitated calcite,

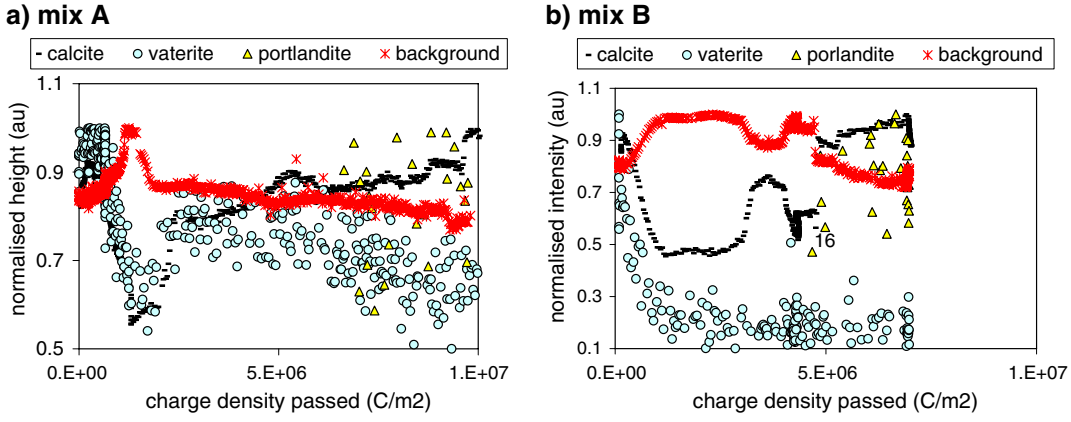

Fig. 12. (a–b): Evolution of the normalized background and normalised heights for calcite, vaterite and portlandite, as a function of the charge density passed for a) mix A and b) mix B.

some vaterite and without portlandite. The amount of calcium in solution is that allowed by the solubility of the calcite.

At the cathode, electrolysis of water takes place, with evolution of hydrogen and production of hydroxyl ions. This reaction takes place at the rebar. Therefore, when the electrical field is applied, according to Faraday's law, each 96 486 C of current passed imply the decomposition of one molecule of water and the formation of one equivalent of OH^- at the cathode. Therefore, there is a slight reduction in the background due to the loss of water and release of H_2 through the porous network of the paste. On the other hand, there is a precipitation of calcite, due, on one hand, to the loss of water, and on the other hand, to the increase in the pH, that diminishes their molar solubility. (see Fig. 12).

When the electroosmotic flux is established, there is a massive entrance of the carbonate solution into the specimen, with a specific pH (about 10.9 and 11.3, respectively for mix A and B, as it was explained before) that, as a first effect, implies the dissolution of calcite and vaterite precipitated by a dilution effect. In addition, the effects of common ion and lower pH of the solution will probably act in the same direction of dissolution of phases. At this point, the background is at the highest point and calcite at its lowest point (see Fig. 12).

The background remains high until water starts to be removed at the same time that it gets more alkaline due to the electrodic reactions. This causes again the precipitation of calcite, and therefore their height increases. Concerning vaterite, it seems that it has lesser tendency than calcite to be formed again after having been dissolved (its solubility is higher in all the range of pH). In fact, for mix A some vaterite remains; however, in the case of mix B, after being dissolved, no new precipitation of vaterite can be observed.

This behaviour is repeated in cycles every time that the electroosmotic flux is produced.

In the other parts of the specimen, there are also simultaneous changes: As explained, calcite has been dissolved and there has been complete disappearance of vaterite in the positive side, liberating Ca^+ ions that are driven, by the electrical field towards the negative electrode. Therefore, when the pH reaches 12.3, there is a precipitation of portlandite, starting at the level of the rebar and progressively extending through the rest of the specimen, as it is illustrated in Fig. 6.

Precipitation of portlandite in the rebar by the application of electrical current had been reported previously by [14] by application of an electrical treatment on alkaline specimens as a preventive measure to increase the layer at the steel-concrete interface but not in carbonated specimens during a realkalisation treatment. The experimental observation of the restoration of the alkaline reserve during a realkalisation process has not been found in the literature.

On the other hand, the dissolution of phases in the positive side explains the increase in porosity noticed, while precipitation of other phases, as portlandite and calcite in the capillary pores of the negative part of the specimen, leads to the decrease of the porosity, in agreement with [15,16].

5. Conclusions

The conclusions that can be drawn up from this research are:

1. It has been possible to in-situ monitoring the electroosmotic flux, during realkalisation, by neutron diffraction. This was achieved by designing the experimental set-up in a way to take profit of the incoherent scattering of the H of the water. The analysis of soluble carbonates in the specimen, after the experiment have confirmed the electroosmotic flux as a driving force of the realkalisation treatment.
2. For both experiments (CEM I paste and CEM I+FA paste), the whole part of the specimens between both electrodes has turned pink with the phenopthaleine indicator, which means success in the realkalisation treatment.
3. For the two mixes tested (CEMI and CEM I+FA paste), most of the relevant electroosmotic phenomena take place in the range of pH of the anolyte between 10.5 and 11.5.
4. The averaged values of zeta-potential, calculated from the averaged electroosmotic flux, for mixes A and B have been of −1.2 and −4 mV, respectively. Therefore, the zeta potential of the electrical double layer in the walls of the pores of cement paste is more negative when adding fly ashes to the clinker than when using plain CEM I.
5. There is precipitation of portlandite on the rebar and on the zone close to the negative electrode as far as the pH is high enough. The provision of Ca^{2+} ions comes from the dissolution of calcite and vaterite. So, it is possible to restore the alkaline reserve if passing enough amount of charge. Once dissolved, calcite precipitates again in function of the dilution and pH conditions. However, once vaterite decomposes, no new formation takes place.
6. The dissolution of phases in the positive side implies a higher porosity while precipitation of other phases, as portlandite and calcite, in the negative part of the specimen can even lead to the decrease of the porosity in the surroundings of the rebar.

Acknowledgements

The experiments reported here were done thanks to the beamtime (Exp 5-25-48) granted by the Institute Max von Laue-Paul Langevin (ILL). The authors are especially grateful to the staff of D20. The authors also acknowledge the funding provided by the Spanish MMA through the project n° 055/2004/3.

References

[1] R. Polder, H.J. Van Der Hondel, Electrochemical realkalisation and chloride removal of concrete. State of the art, laboratory and field experience, Proc. of RILEM Conference 'Rehabilitation of Concrete Structures' Melbourne, 1992, pp. 135–147.
[2] Ø. Vennesland, Proc. Nordisk Beton Kongress, Odense, Senmark, 1987.
[3] J.B. Miller, Structural aspects of high powered electro-chemical treatment of reinforced concrete, in: R.N. Swamy (Ed.), Proceedings of the International Conference on Corrosion and Protection of Steel in Concrete, 24–28 July, Sheffield Press, 1994.

[4] R. Polder, 'Electroosmosis in Concrete. Theory, Basic and Field Data and Preliminary Tests', TNO-report 93-BT-R1423, .
[5] P.F.G. Banfill, Features of the mechanism of realkalisation and desalination treatments for reinforced concrete, Proceedings of the International Conference on 'Corrosion and Protection of Steel in Concrete', 24–28 July, Sheffield Press, 1994.
[6] R.J. Hunter, Zeta Potential in Colloid Science. Principles and Applications, Academic Press Limited, 1981.
[7] C. Andrade, M. Castellote, J. Sarría, C. Alonso, Evolution of pore solution chemistry, electro-osmosis and rebar corrosion rate induced by realkalisation, Materials and Structures 32 (1999) 427–436.
[8] M. Castellote, I. Llorente, C. Andrade, Influence of the external solution in the electroosmotic flux induced by realkalisation, in: Mater. Construcc., vol. 53, no 271–272, 2003, pp. 101–111.
[9] T. Chaussadent, G. Arliguie, AFREM test procedures concerning chlorides in concrete: Extraction and titration methods, Materials and Structures 32 (217) (1999) 230–234.
[10] Goñi, S, Alonso, C., Menendez, E., Hidalgo, A., Andrade, C. "Microstructural characterization of the carbonation of mortar made with fly ashes" Proceedings of the 10th International congress on the chemistry of cement, Gothenburg, Sweden, June, 1997, vol. 4, Performance and durability of cementitious materials, 4iv004, 8 pp, Edited by Harold Justnes, Trondheim, Norway, Published by Amarkai AB, Goteborg, Sweden, 1997.
[11] Bennet, J.E., Schue, T.S, "Electrochemical chloride removal from concrete". A SHRP Contract Status Report. Corrosion 90, Las Vegas, Nevada, Paper n° 316, April, 1990.
[12] M. Castellote, C. Andrade, C. Alonso, Modelling of the processes during steady-state migration tests: quantification of transference numbers, Materials and Structures 32 (April 1999) 180–186.
[13] M. Castellote, C. Andrade, C. Alonso, Electrochemical chloride extraction: influence of testing conditions and mathematical modelling, Advances in Cement and Research 11 (2) (Apr. 1999) 63–80.
[14] G.K. Glass, N.R. Buenfeld, The inhibitive effects of electrochemical treatment applied to steel in concrete, Corrosion Science (2000) 923–927.
[15] M. Castellote, C. Andrade, C. Alonso, Changes in the concrete pore size distribution due to electrochemical chloride migration trials, ACI Materials Journal (96-M39) (May/June 1999) 314–319.
[16] M. Castellote, X. Turrillas, C. Andrade, C. Alonso, A. Kvick, A. Terry, G. Vaughan, J. Campo, Synchrotron Radiation Diffraction Study of the microstructure changes in cement paste due to accelerated leaching by application of electrical fields, Journal of American Ceramic Society 85 (3) (2002) 631–635.